Draft version December 25, 2016
Preprint typeset using LaTeX style AASTeX6 v. 1.0

# CHARACTERIZING THE COMPLEXITY EVOLUTION OF GAMMA-RAY BURST PULSES

Eric Hofesmann
Department of Physics and Astronomy, College of Charleston

Advisor: Jon Hakkila
Associate Dean of the Graduate School and Professor of Physics and Astronomy Graduate School, University of Charleston, S. C.
Campus Director, South Carolina NASA Space Grant Consortium

(Dated: December 14, 2016)

## ABSTRACT

NASA's Burst And Transient Source Experiment (BATSE) Gamma-Ray Burst catalog was used to analyze complex Gamma-Ray Burst pulses. Complex GRB pulses are selected based off of the condition that there is an unknown number of pulses due to high variability in the structures intensity or due to non standard residual structures. Once the sample is selected, the pulses are scaled based off of their amplitude, asymmetry, and duration. The pulse intensities of the scaled pulses were interpolated to allow the pulses to be added together. The summed pulses were then binned to run through an existing pulse fitting algorithm. The pulse fit was removed from the data and the residuals were examined using another algorithm. Complex pulses were found to have similar characteristics within subgroups of bursts.

Contents

## 1. INTRODUCTION

Gamma-Ray Bursts (GRB) are observed as emissions of gamma radiation originating from the most powerful events in the universe (Hakkila et al. 2015). They were first discovered during the 1970's while the United States government was searching for radiation emissions from Soviet nuclear tests (Klebesadel et al. 1973). They were assumed to be galactic in nature but the distribution of bursts proved that they were in fact cosmological (Metzger et al. 1997). Theories as to what causes them are currently incomplete (Norris et al. 2005). The current leading theory assumed the progenitors of GRB emission to be relativistic shocks with enough energy to create gamma-rays in only a matter of seconds (Rees & Meszaros et al. 1992). GRB emission contains a prompt high energy emission followed by an afterglow of steadily decreasing energy which can last from a few minutes up to several days (Costa et al. 1997). This afterglow begins in the X-ray wavelengths and moves to radio wavelengths as the progenitor cools (Costa et al. 1997). GRB prompt emission are classified by their most basic structures, the GRB pulse, which was originally characterized by an asymmetric monotonic increase and decrease, a broadening in lower energy channels, and a hard to soft spectral evolution (Hakkila et al. 2011) (Norris et al. 1997). However, research has shown that GRB pulses in fact contain two peaks in addition to the main peak, one on the rise and one on the decay (Hakkila & Preece et al. 2014). At each peak, a re-hardening occurs within the pulse (Hakkila & Preece et al. 2014). While there is this general structure found among most pulses, some are difficult to identify often due to overlapping pulses and low signal to noise.

Even though the true origins of GRBs are unclear, GRB data have been collected for decades (Hakkila et al. 2015). One of the most prominent data collection projects was the Burst and Transient Source Experiment, BATSE, launched on board NASA's Compton Gamma-Ray observatory in 1991 (Paciesas et al. 1999). BATSE recorded the counts of gamma-ray photons coming into its detectors in 64 ms time bins in four different energy channels. These energy channels range from 25 - 50, 50 - 100, 100 - 300, and $>$ 300 keV as shown in Figure 1 (Fishman et al. 1989). Thousands of bursts were recorded over the years that BATSE was operational.

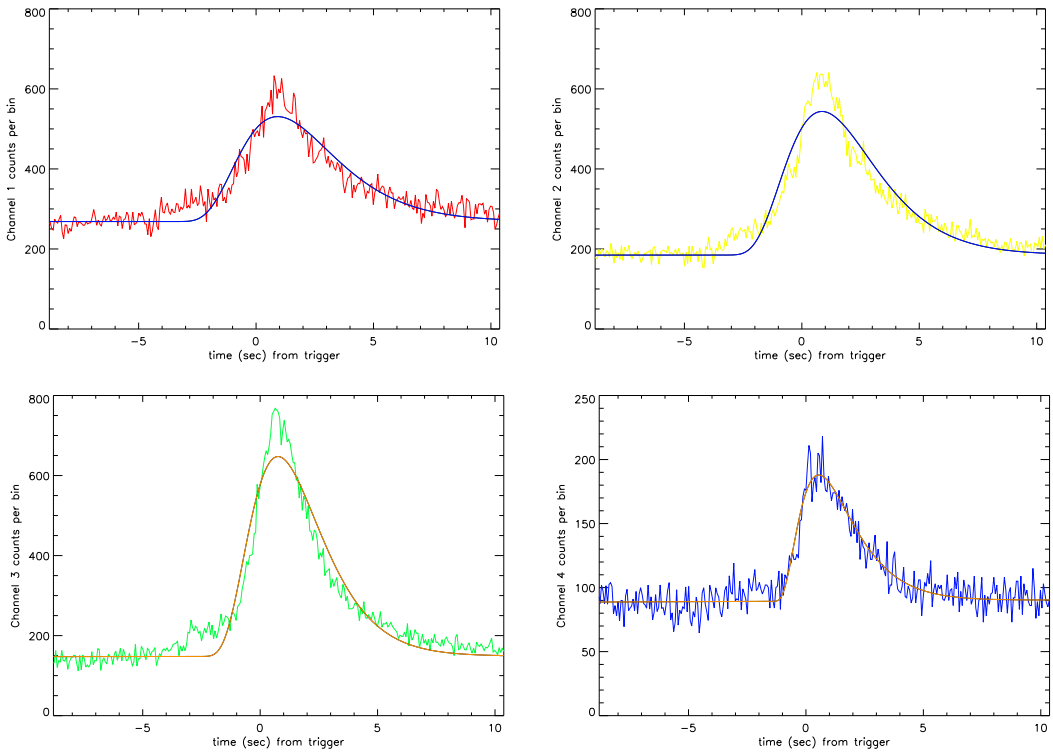


**Figure 1**. The photon counts of various channels recorded by BATSE in trigger 3954. The top left red plot is the first and lowest energy channel ranging from 25 - 50 keV. The top right yellow plot is the second energy channel containing energies ranging from 50 - 100 keV. The bottom left green plot is the third energy channel containing energies ranging from 100 - 300 keV. The bottom right blue plot is the fourth energy channel containing all energies greater than 300 keV.

GRB pulses often share similar characteristics like the three peak structure and a hard to soft evolution (Hakkila &

Preece et al. 2014). However, many variations of complex gamma-ray bursts exist which are defined by our inability to discern the number of underlying pulses within each burst or by a non standard residual structure. The sample of complex pulses used in this research can be found in the Appendix. There is reason to believe that in some instances, even though a single emission shows what appear to be multiple pulses with high fluctuations in intensity, it can still be considered a single pulse. During his time at the College of Charleston, Thomas Cannon was also an undergraduate research student working with Dr. Jon Hakkila. Through his pulse fitting process, he found a class of GRB pulses that we came to call Crowns. The properties of Crowns are a symmetric pulse structure with a sharp rise and decay along with a noisy peak to give them a crown-like shape. These pulses have caused problems in the creation of a catalog of fitted pulses since the underlying structure present in these complex Crowns could not be identified.

## 2. PULSE FITTING ALGORITHMS

### 2.1. *Norris Pulse Fitting Algorithm*

GRB pulses have been historically modeled to be monotonically increasing and decreasing with only a single peak. Many different simple models have been developed. The Norris et al. (2005) model was used over other models because it used only 4 parameters as opposed to 5, 6, or more (Hakkila et al. 2015). This is important because any kind of pulse could be fit given enough free parameters which does not allow for accurate analysis of the model. The Norris et al. (2005) model is a function of intensity with respect to time.

$$I(t) = A\lambda \exp^{[-\tau_1/(t-t_s)-(t-t_s)/\tau_2]} \tag{1}$$

All times are measured in seconds. The four parameters are the amplitude $A$, the start time $t_s$, and two variables related to the rise and decay, $\tau_1$ and $\tau_2$. Where $\lambda = Exp[2(\tau_1/\tau_2)^{1/2}]$ and the peak of the pulse occurs at time $\tau_{peak} = t_s + \sqrt{\tau_1\tau_2}$ (Norris et al. 2005). In addition, an important characteristic in modeling a pulse is the fiducial timescale (Hakkila et al. 2015). This timescale is measured by whenever the pulse intensity drops to some $e^{-n}$ of its maximum amplitude. A value of $n = 3$ represents an intensity of 4.98% of the maximum amplitude (Hakkila & Preece et al. 2014). In this experiment a value of $n = 5$ was used to preserve more of the data. The duration of the fiducial timescale is given by $w$ which is composed of the rise time, $\tau_{rise}$, and the decay time, $\tau_{decay}$ (Hakkila & Preece et al. 2014)

$$\tau_{rise} = \frac{n\tau_2}{2}[\sqrt{1 + 4\mu/n} + 1] \tag{2}$$

$$\tau_{decay} = \frac{n\tau_2}{2}[\sqrt{1 + 4\mu/n} - 1] \tag{3}$$

$$w = \tau_{rise} + \tau_{decay} = n\tau_2\sqrt{1 + 4\mu/n} \tag{4}$$

Where $\mu = \sqrt{\tau_1/\tau_2}$ (Hakkila & Preece et al. 2014). An example of the Norris et al. (2005) model fit onto a GRB pulse can be seen in Figure 2.

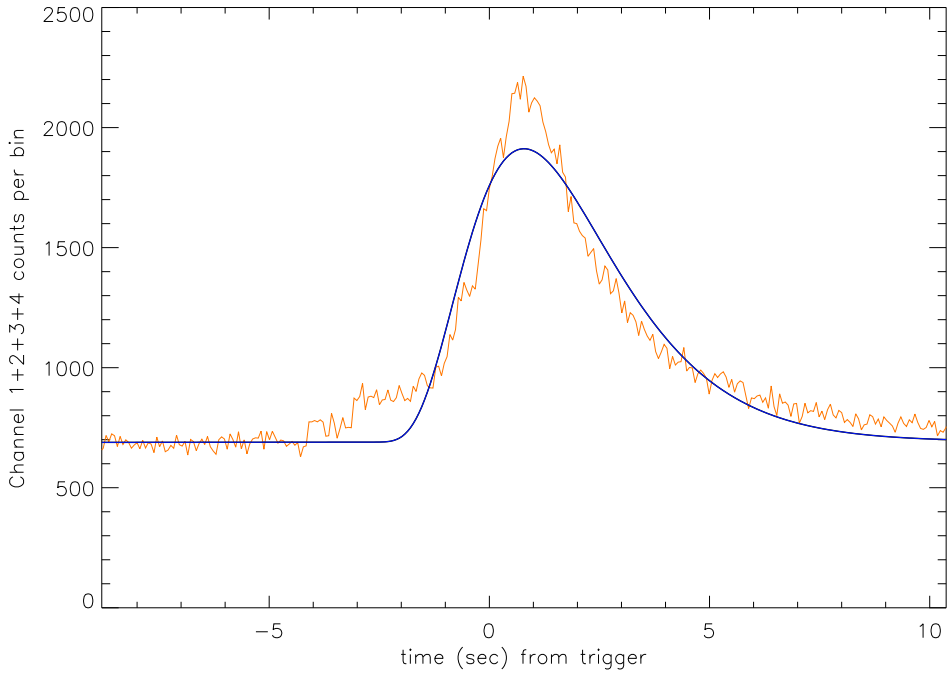


**Figure 2**. BATSE trigger 03954: 64 ms data shown in orange with the Norris et al. (2005) pulse model plotted on top of it in blue.

Software has been developed that uses Bayesian statistics and a nonlinear least squares fitting routine to accurately fit the parameters of the Norris et al. (2005) model to a given BATSE light curve (Hakkila et al. 2008). In summary, the way that this code functions is that it breaks apart the light curve into various Bayesian blocks (Scargle et al. 1998) that are of statistical significance (Hakkila et al. 2008). Each of these blocks is defined to be between two change points. Once these blocks are identified, the function MPFIT is incorporated to attempt to fit a Norris et al. (2005) model within each of the Bayesian blocks using a built in nonlinear least squares fitting routine. The $\chi^2$ per degree of freedom is then optimized by combining the Bayesian blocks together and attempting a fit once again. Once this ideal $\chi^2_{dof}$ is found, the Norris et al. (2005) model parameters and their corresponding uncertainties are saved to a text file (Hakkila et al. 2011).

User training is required when fitting GRB pulses using this method. Parameters such as a log value for the number of initial change points, the standard deviation above background that defines statistical significance, and the timescale that is being examined can be altered on a pulse by pulse basis. Each pulse can be fit in a different way and thus these parameters can vary greatly in order to fit one pulse over another. These parameters are important because they will limit the number of Bayesian blocks that the program finds. If the parameters are set too low, then multiple pulses will be fit to what is clearly a single pulse. However, if the values are set too high, then the program fails to find a pulse of statistical significance.

### 2.2. *Residual Fitting Algorithm*

After extensive research, imperfections in the Norris et al. (2005) model were found to occur in a predictable and reproducible pattern which results in the form of three peaks as mentioned before (Hakkila & Preece et al. 2014). These discontinuities could be picked out by subtracting the Norris et al. (2005) model fit from the data and plotting the residuals as seen in Figure 3. The Hakkila & Preece et al. (2014) model for these residuals is a four parameter function of time:

$$\mathrm{res}(t) = \begin{cases} AJ_0(\sqrt{\Omega[t_0 - t - \Delta/2]}) & \text{if } t < t_0 - \Delta/2 \\ A & \text{if } t_0 - \Delta/2 \leq t \leq t_0 + \Delta/2 \\ AJ_0(\sqrt{s\Omega[t - t_0 - \Delta/2]}) & \text{if } t > t_0 + \Delta/2 \end{cases} \tag{5}$$

$J_0(x)$ is the integer Bessel function of the first degree. The four parameters are the time of the central peak $t_0$, the amplitude of the normalized plateau peak $A$, the angular frequency of the Bessel function $\Omega$, the scaling factor in front of and behind the peak $s$, and the duration of the peak plateau $\Delta$ (Hakkila et al. 2015). This plateau was incorporated due to the duration of the main residual peak. If this parameter is discarded then the main peak would be too sharp to be an accurate fit. Empirical testing shows that this value is on average 0.01 and can be assumed as such, thus reducing the parameters to four. (Hakkila et al. 2015).

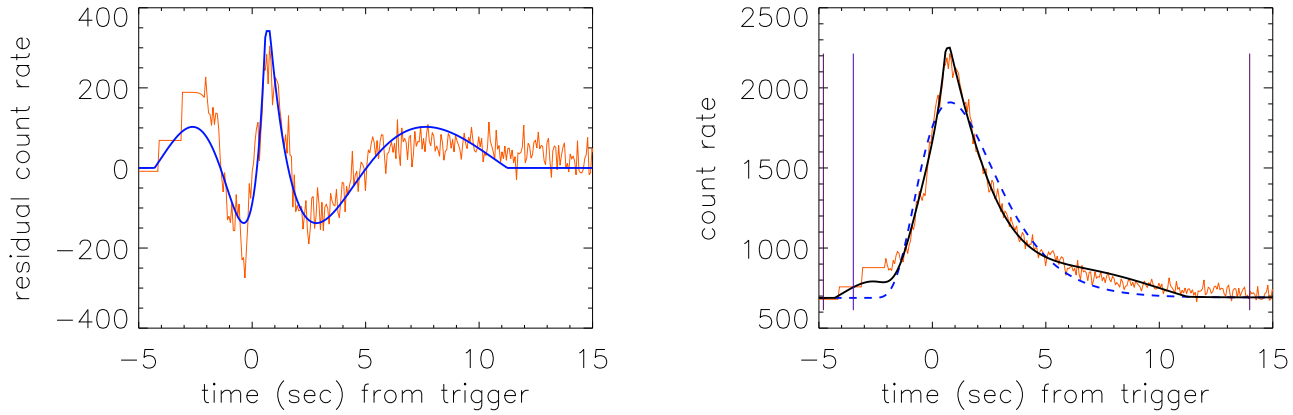


**Figure 3**. BATSE trigger 03954: The Norris et al. (2005) pulse model fit is the dotted line shown on the right. The left plot shows the Norris et al. (2005) fit on the right subtracted from the trigger data on the right. The Hakkila & Preece et al. (2014) residual model fit is shown in blue on the left. The black line on the right graph represents the Hakkila & Preece et al. (2014) residual model and the Norris et al. (2005) model added together. The left most and right most lines on the right graph show the fiducial start and stop times.

This Bessel function based fit was chosen due to its time reversibility and because of the few parameters it requires. However, it only serves as an empirical model. Errors in this Hakkila & Preece et al. (2014) residual model can be seen when applied to bright pulses with high signal to noise. The true shape of a GRB pulse emerges and the Hakkila & Preece et al. (2014) residual model has difficulty fitting it as seen in Figure 4.

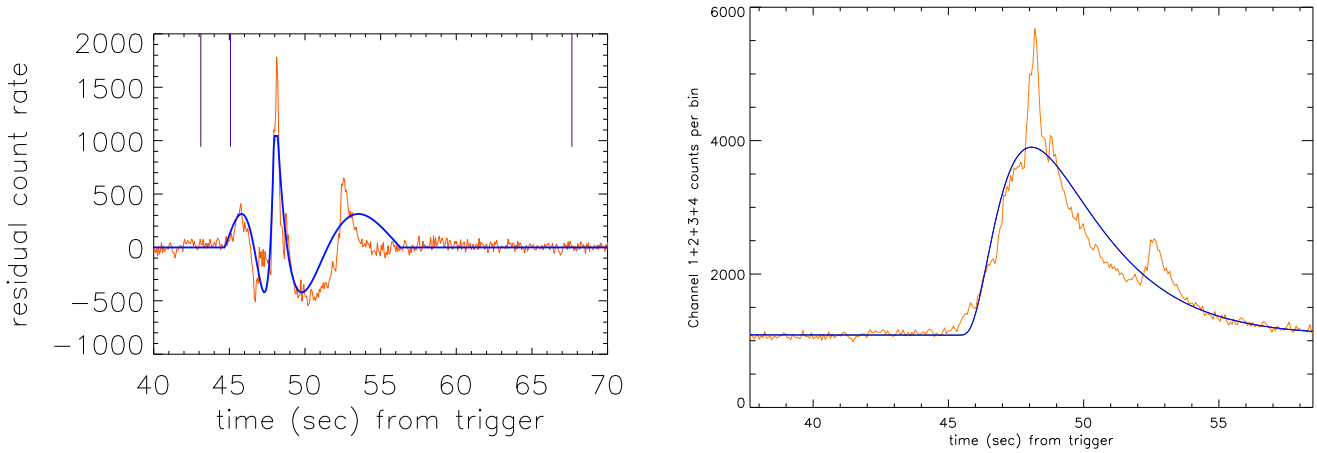


**Figure 4**. BATSE trigger 00143: The Norris et al. (2005) pulse model fit is the blue line shown on the right. The left plot shows the Norris et al. (2005) fit on the right subtracted from the trigger data on the right. The Hakkila & Preece et al. (2014) residual model fit is shown in blue on the left.

The goal of this research experiment was to identify complex Gamma-Ray Burst pulses, specifically Crowns, and combine their intensities to examine underlying structures present across the collected data set. The inception of this project began during the creation of a BATSE GRB pulse catalog where several pulses were found that had

residuals defying the current model and expectations. Some pulses that showed a single emission contained more than three residual peaks. This brought up the hypothesis that there may be some structure that cannot easily be seen in complex pulses that gets diminished in a standard pulse. Pulses have been found that seem to show intermediate steps between a standard three peaked pulse and a complex pulse by clearly having multiple residual peaks. As you can see in Figure 5, there are an additional two peaks on either side of the main peak along with the standard precursor and decay peaks (Hakkila & Preece et al. 2014)

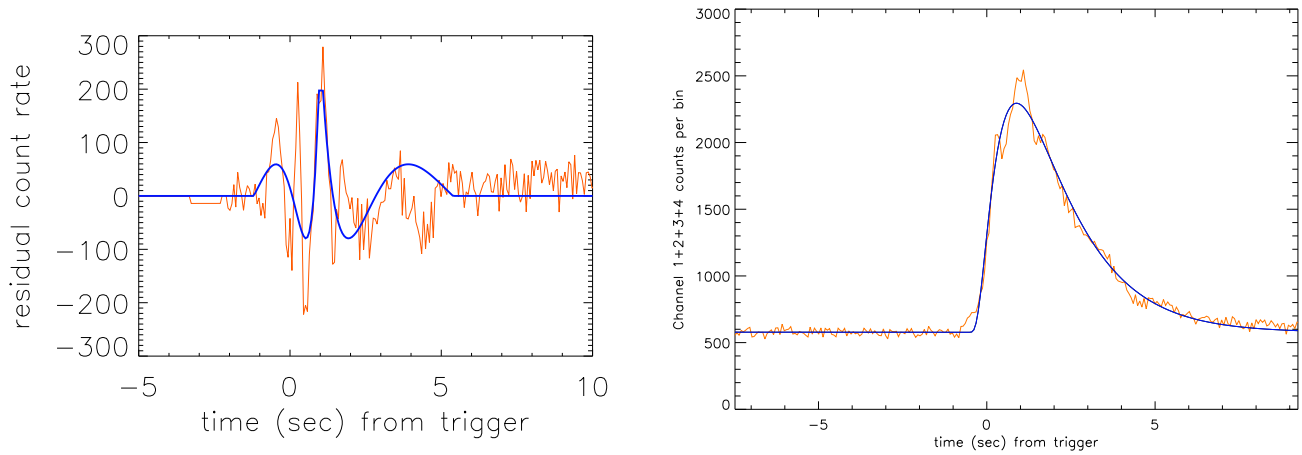


**Figure 5**. BATSE trigger 05417: The Norris et al. (2005) pulse model fit is the blue line shown on the right. The left plot shows the Norris et al. (2005) fit on the right subtracted from the trigger data on the right. The Hakkila & Preece et al. (2014) residual model fit is shown in blue on the left. The left most and right most lines on the left graph show the fiducial start and stop times.

## 3. METHODS

### 3.1. *Pulse Selection*

The first stage of this research project was to use the BATSE database (Paciesas et al. 1999) to analyze pulses that show a complexity in structure that currently renders them unusable and organize them into a data set. An unusable pulse is a complex one in which the number of pulses cannot confidently be determined or the residual structure not adhering to the norm. Various samples were selected including Crowns and other complex pulses that contain multiple peaks. These were selected by examining the pulse structures and hand selecting appropriate bursts. The options in pulses to choose from were fairly sparse since the pulse not only had to be complex, but it also had to be bright enough to contain statistically significant residuals and it needed to be a single emission episode. Many complex bursts consist of various spikes that continue for up to a minute or more at times. As seen in the Appendix, some of the complex pulses that were chosen do in fact consist of various spikes and can take up to a minute, however, they were only selected because their grouping showed the possibility of a single underlying pulse. The samples that were chosen were broken up further into three categories: 48 complex pulses, 27 Crowns, and a subset of 13 of the 27 Crowns. The 48 complex pulses were selected to incorporate a range of complexity and so do not include all 27 Crowns. Generally, the brightest pulses were sought out as these are able to better show structure differentiated from the background noise.

### 3.2. *Pulse Scaling*

After the data sets have been selected, all pulses needed to be scaled to the same asymmetry, amplitude, and duration. If they were not, then the bright and long pulses would dominate the summed pulse plot. Similarly, since the Hakkila & Preece et al. (2014) residual structures are of great importance, the asymmetry also had to be scaled. Otherwise the residual peaks would not be in the same location from one pulse to another with respect to the peak time, $\tau_{peak}$, and as a result they could cancel each other out. This scaling was done by using the fiducial timescale as mentioned previously (Hakkila & Preece et al. 2014). The fiducial start time was set to $-1$ seconds and the fiducial end time was set to 1 second. The asymmetry was then scaled so that the peak time was at 0 seconds. This was done by subtracting the peak time and dividing the fiducial start time from every time point in the pulse data. The amplitude was scaled by dividing every counts point by the value of the maximum counts of the pulse. One issue that

may occur from this is that the pulse fitting program has difficulty fitting very symmetric pulses. For the pulse to be symmetric, $\tau_1$ must be orders of magnitude larger than $\tau_2$. Thus, the start time, $t_s$, will be set to a value that is much smaller than where the pulse actually begins. The equation that calculates the peak time, $\tau_{peak}$, incorporates $t_s$, $\tau_1$, and $\tau_2$, causing this issue. For this experiment, this value is only used to create a fit for the data, thus it is not crucial for it to be exact, however, since the value is very small, any variation in it will cause the program to behave differently.

One issue that arises is that all pulses have different durations and thus if scaled, will then have different resolutions. In order to be able to sum pulses together, they need to include the same number and values of time data, which will no longer be at a 64ms resolution after the scaling. Also, the part of the pulse before and after the peak will be scaled differently for asymmetry and thus have different resolutions. For all pulses to incorporate the same time values, their intensities need to be interpolated at the time values that are not included in the pulse data (Hakkila & Preece et al. 2014). For this to be accomplished, the time data of every pulse were added into an array. From here, every time value that was not already included within the 64ms timescale of a pulse was then interpolated using the two nearest time points and their corresponding intensities. A linear interpolation was used as it is the most direct method of averaging two values. In the end, each pulse contains the same number of time values where no two time values are separated equally.

### 3.3. *Summed Pulse Fit and Residuals*

Once the scaling was complete, the pulses could be added together at each time value with the corresponding interpolated intensity values. The residuals of this summed pulse then needed to be extracted. For this to occur, this data needed to be read into the original Norris et al. (2005) model fitting program (Hakkila et al. 2008). However, this program inputs the time scale as 64ms at an evenly spaced resolution. Thus the summed pulse then needed to be binned. The binning was accomplished by starting at the peak time, then moving down the pulse in both directions in a certain increment. This increment was calculated by finding the average number of bins within a pulse's fiducial timescale at a 64ms resolution. In this case, the average fiducial duration was taken to be 10 seconds. As the incremental region moved down the pulse, any intensity values within this region were averaged together to produce a single value. Finally, the Norris et al. (2005) model fitting program was able to read the summed pulse data and produce the corresponding fit to it.

The residuals could then be taken and analyzed in relation to one another. If peaks form in this summed residual data, then this implies that there is an underlying structure that is prevalent among the majority of pulses. The flatter the sum of these pulses, the less of a structural relationship these pulses have. A peak in this summed plot can be quantified through the statistical analysis of it compared to other fluctuations in the plot. If there is no significant statistical result from the plot then this implies that the residual structures of complex pulses do not follow the temporal structures of standard pulses.

## 4. RESULTS

The results of the summed pulses can be visually inspected in Figure 6. These images show the outcome of scaling together and adding 48 varying complexity pulses, 27 Crowns, and a subset of 13 of those 27 Crowns. What these results show is that there are slight variations in the rise and decay of the 48 summed pulses. There are slightly larger variations in the summed 27 Crowns. Then in the summed 13 Crowns, there are very clearly five separate peaks.

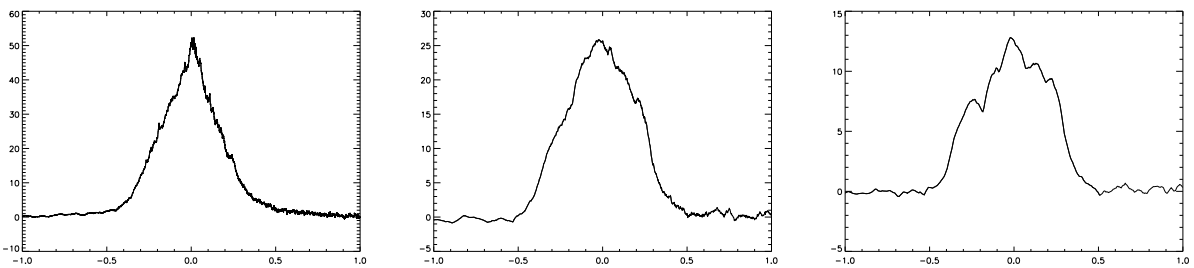

**Figure 6**. The left most graph is the sum of all 48 complex pulses shown in Figure 12 in the Appendix. The middle graph is the sum of all 27 Crown pulses shown in Figure 13 in the Appendix. The right most graph is the sum of the first 13 Crown pulses shown in Figure 13 in the Appendix. All of these plots were scaled so the peak time was at 0, the fiducial start time was at $-1$, and the fiducial end time was at 1.

These pulses were then fit to the Norris et al. (2005) model using the Bayesian block and nonlinear least squares fitting routine mentioned previously (Hakkila & Preece et al. 2014). This fit was then subtracted from the summed pulse data resulting in the residual structures shown in Figures 7, 8, and 9.

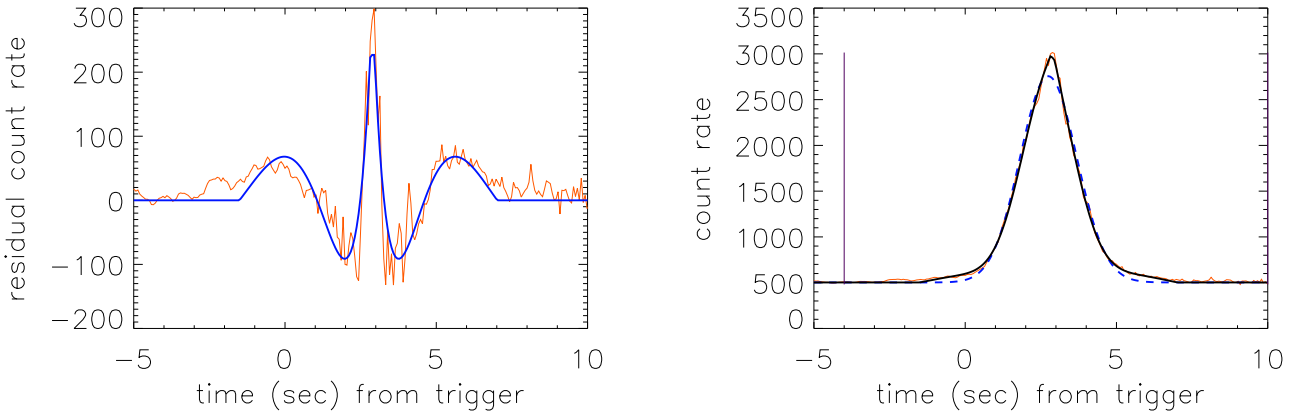


**Figure 7**. 48 Complex Pulses Summed: The Norris et al. (2005) pulse model fit is the dashed line shown on the right. The left plot shows the Norris et al. (2005) fit subtracted from the trigger data on the right. The Hakkila & Preece et al. (2014) residual model fit is shown in blue on the left. The time on the x-axis can be disregarded since the summed pulse has been binned.

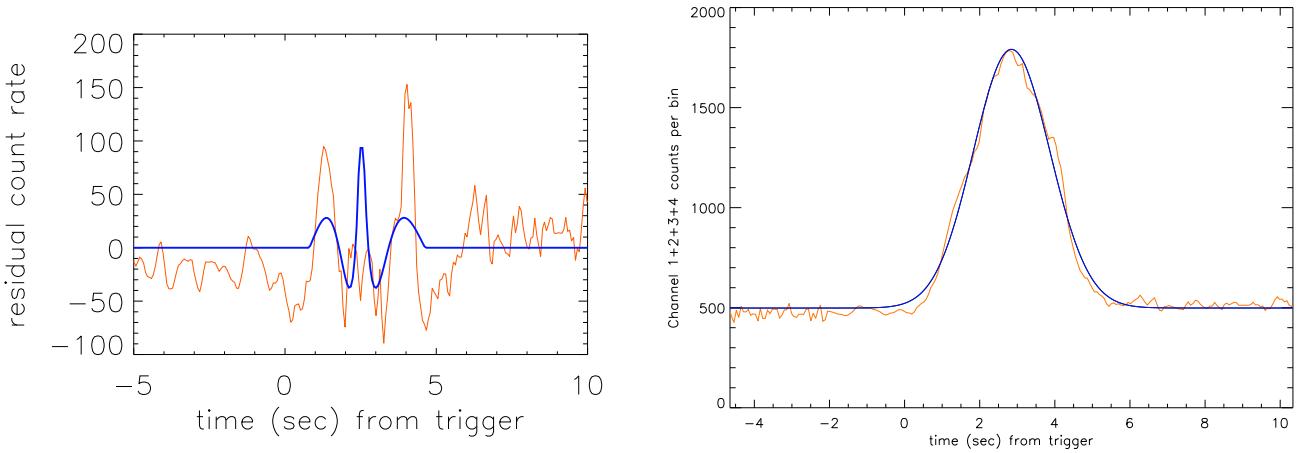


**Figure 8**. 27 Complex Crown Pulses Summed: The Norris et al. (2005) pulse model fit is the dashed line shown on the right. The left plot shows the Norris et al. (2005) fit subtracted from the trigger data on the right. The Hakkila & Preece et al. (2014) residual model fit is shown in blue on the left. The time on the x-axis can be disregarded since the summed pulse has been binned.

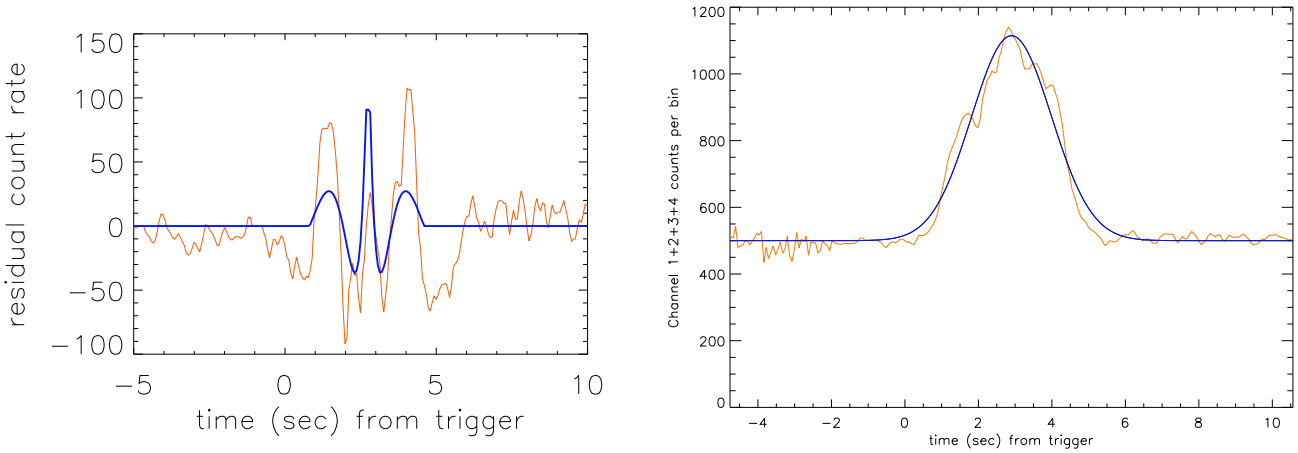


**Figure 9**. 13 Complex Crown Pulses Summed: The Norris et al. (2005) pulse model fit is the dashed line shown on the right. The left plot shows the Norris et al. (2005) fit subtracted from the trigger data on the right. The Hakkila & Preece et al. (2014) residual model fit is shown in blue on the left. The time on the x-axis can be disregarded since the summed pulse has been binned.

To distinguish if the residual structures that were found are real, they needed to be compared to the background noise (Hakkila & Preece et al. 2014). This was done by taking a sample of the summed background of the pulse and finding the variance therein. This variance was then compared with that of where the residual structures lie. If there was a significant difference, then the residual structures are real. These variances are shown in Table 1.

**Table 1**. Variance of Residual Data

| Summed Pulse | Background Variance | Residuals Variance |
|---|---|---|
| 48 Complex | 142.37720 | 4221.0859 |
| 27 Crowns | 369.44476 | 3452.4415 |
| 13 Crowns | 117.92508 | 2462.2639 |

Since the Hakkila & Preece et al. (2014) residual structure shown in Figure 9 appears to have five residual peaks, the residual function was altered in an attempt to account for this. As mentioned previously, the Hakkila & Preece et al. (2014) residual model includes the integral Bessel function which continuously propagates in time. Thus it is possible to extend the residual pattern to the following Bessel function peaks for a total of five residual peaks. This is done by changing the Bessel function cutoff to a following zero value where the function crosses the x-axis. The results of this are shown in Figure 10. The pulse was fit with the attempt to align the two additional peaks with those of the Bessel function.

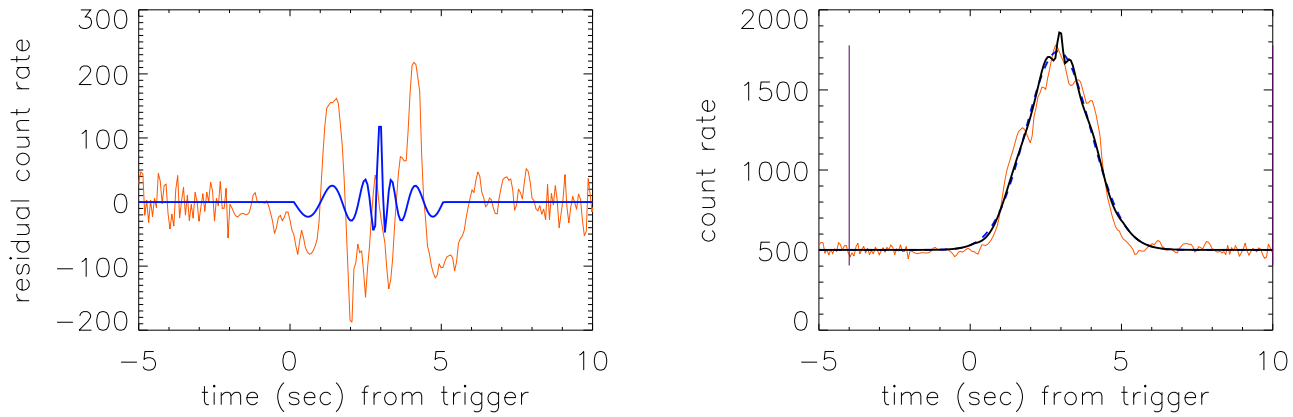


**Figure 10**. 13 Complex Crown Pulses Summed: The Norris et al. (2005) pulse model fit is the dashed line shown on the right. The left plot shows the Norris et al. (2005) fit subtracted from the trigger data on the right. The Hakkila & Preece et al. (2014) residual model fit is shown in blue on the left and has been extended to include an additional peak and trough.

## 5. CONCLUSION

Visually, complex pulses seem to lack any continuously present structure, as can be seen in the Appendix. The results of this project, however, show that there exist various groups of pulses within the range of complex pulses that do exhibit similar characteristics. When all complex pulses were added together, the underlying structure was removed. However, when smaller samples were selected, there are structures that appear. Figure 6 shows that as more pulses are added, more structure gets removed. Thus when only the 13 most similar crowns are added together, a residual structure appears as seen in Figure 9. An interesting note is that even though the summed pulses in Figure 8 and Figure 9 look fairly different from one another, the residual structures of them are similar. This is in part due to the 13 Crowns being a subset of the 27 Crowns, but it also implies that the same residual structures are also present in some fashion in the remaining Crowns. Since the variance of the pulse residuals shown in Table 1 are on the order of ten times larger than the background variance, these residuals can be considered real.

Extending the integral Bessel function is not a viable method in plotting multiple Hakkila & Preece et al. (2014) residual structures. The two additional residual peaks have a much lower amplitude than either the precursor, the main, or the decay peaks. The Bessel function assumes that everything aside from the main peak has a similar amplitude. In addition, the two new peaks are much closer to the main peak than the rise or the decay peak. Thus, this method cannot be used to accurately fit residual structures with only a four parameter Hakkila & Preece et al. (2014) residual model.

## 6. FUTURE WORK

Currently, all pulses were hand picked and chosen based on their visually complex structure. One way to streamline the process of pulse selection is automatically find similar pulses based on similar features. In the case of Crown selection, pulses need to be found that all incorporate a symmetric rise and decay. This can be determined by the relation of $\tau_1$ and $\tau_2$. If $\tau_1$ is around four or more orders of magnitude larger than $\tau_2$, then the pulse includes a sharp rise and sharp decay. However, for this to occur, all pulses need to have a Norris et al. (2005) model fit applied to them. The problem with this is that complex pulses inherently are difficult to fit with a standard Norris et al. (2005) pulse model since they do not abide by the same properties. One example of a pulse that is difficult to fit can be seen in Figure 11. It shows a pulse that appears to have an a asymmetry reverse that of what is expected. The Norris et al. (2005) model is not defined to be able to fit something with this structure.

Once this process is automated, there will be an excess of complex pulses that can be examined. Additional subgroups will then be easy to identify and the underlying summed residuals of them can be analyzed.

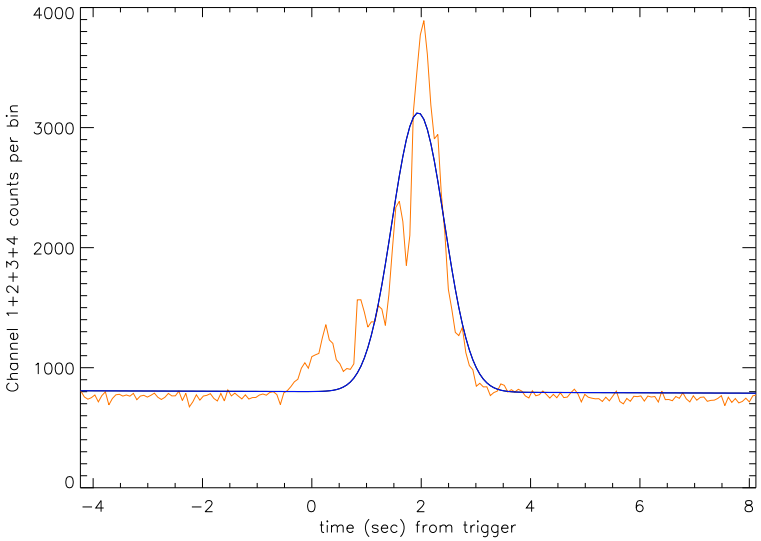


**Figure 11**. BATSE trigger 01025: 64 ms data shown in orange with the Norris et al. (2005) pulse model plotted on top of it in blue.

## 7. ACKNOWLEDGEMENTS

I would like to thank Dr. Jon Hakkila for his advice and mentoring during this project. I would also like to thank Stephen Lesage for the assistance that he has provided throughout this experiment. Finally, I would like to thank Thomas Cannon and Maly Taylor for the catalog of pulse fits that they have supplied.

## 8. APPENDIX

**Figure 12**. BATSE Trigger Numbers for the 48 Pulses used in the complex summed pulse, 00204 00219 00222 : 00249 00503 00537 : 00543 00678 00829:02037 02074 02219:03954 04556 05206 : 05304 05417 05433 : 05436 05447 05471 : 05477 05483 05484 : 05526 05530 05539 : 05547 05567 05568 : 05597 05604 05606 : 05607 05608 05617 : 05621 05629 05637 : 05642 05644 05666 : 05726 05773 05995 : 06422 06621 08027

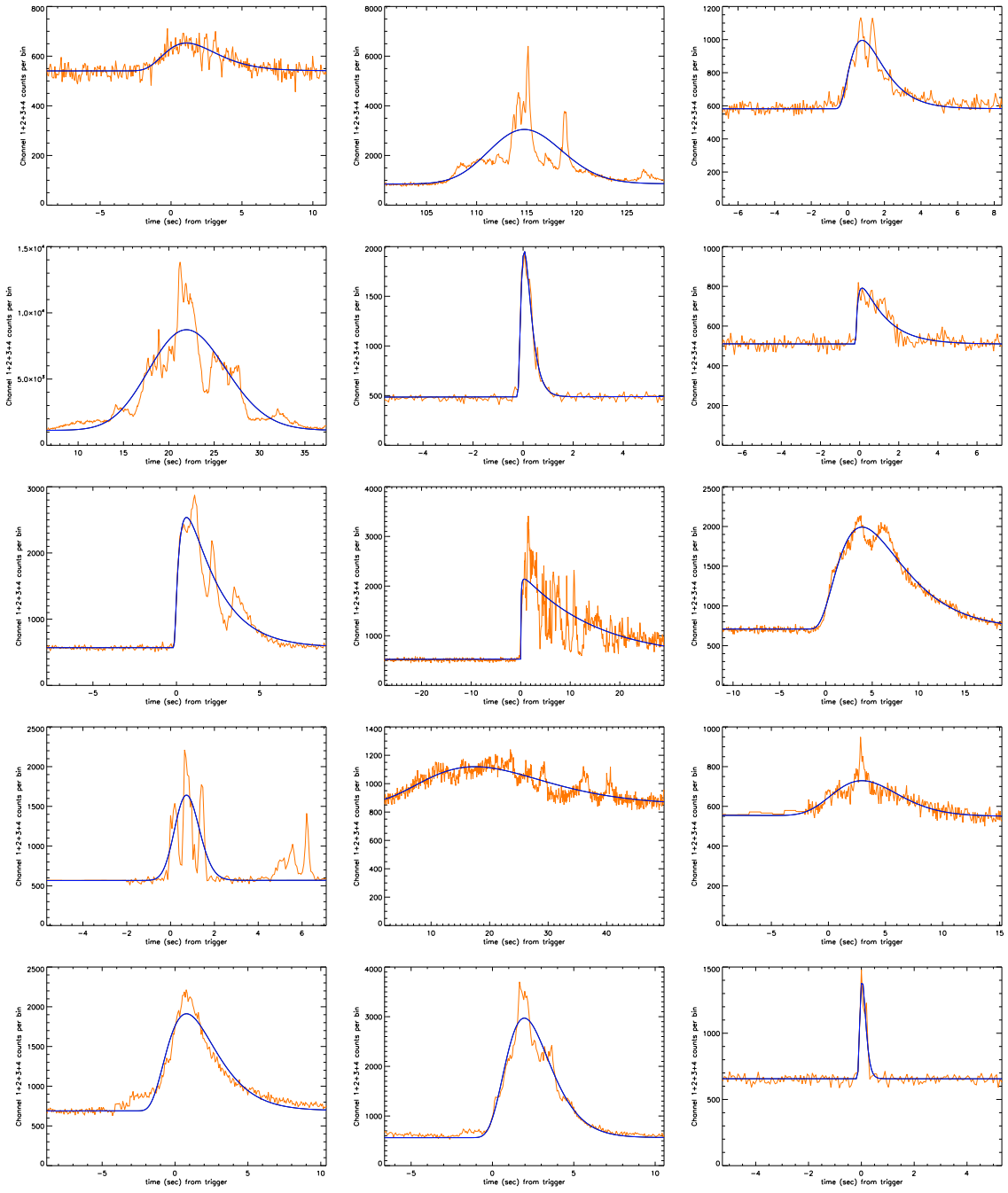

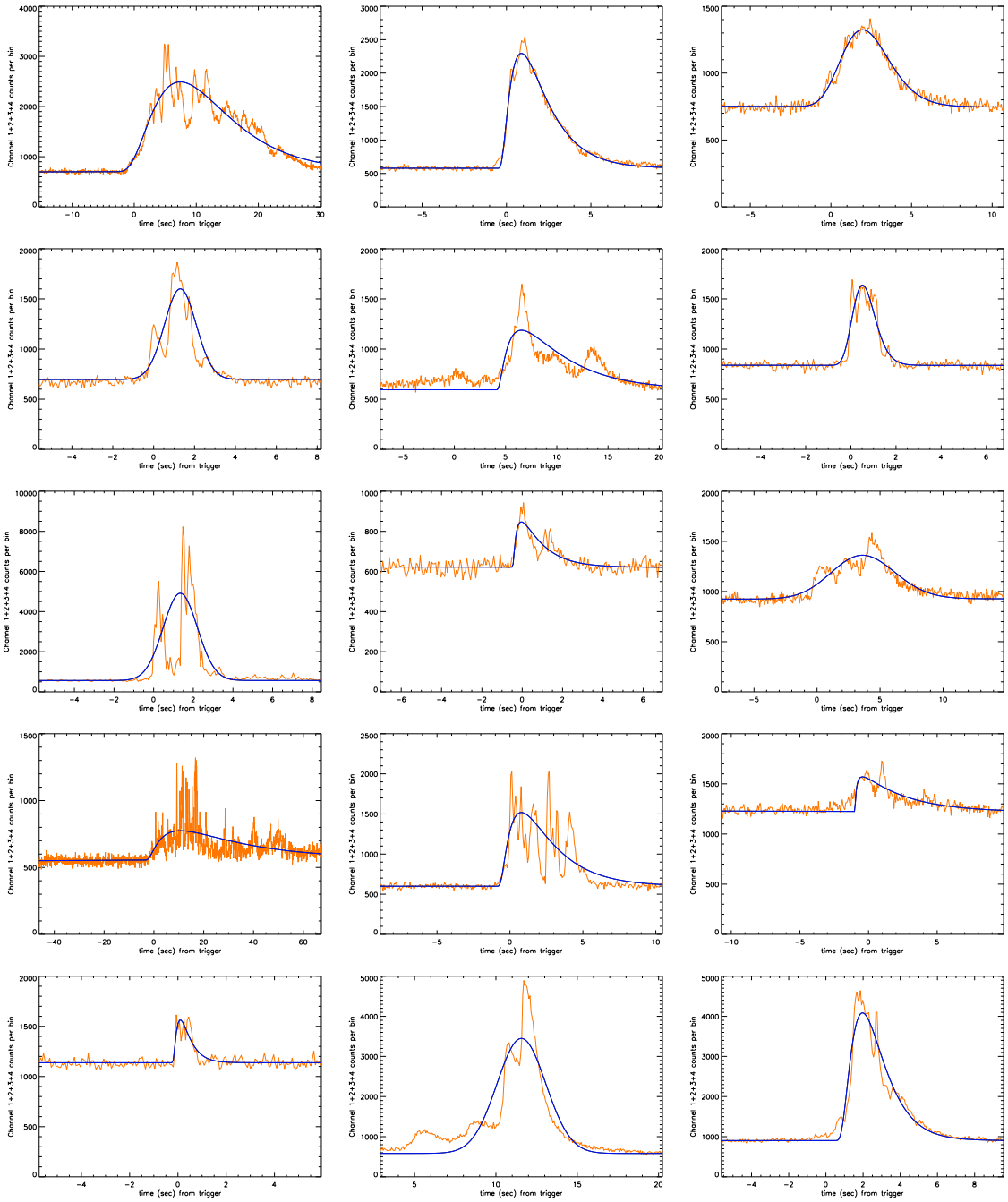
Channel 1+2+3+4 counts per bin
time (sec) from trigger

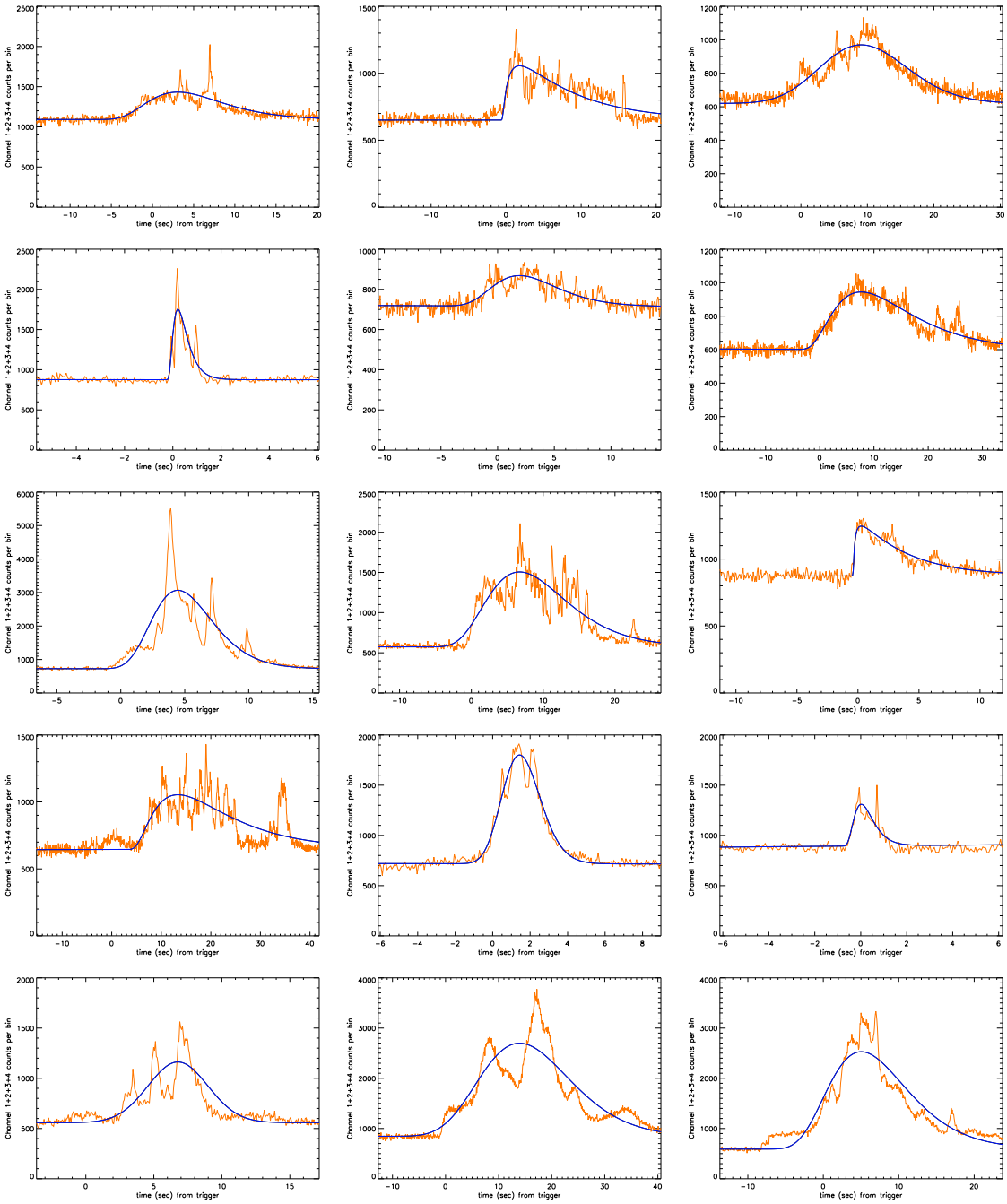
Channel 1+2+3+4 counts per bin
time (sec) from trigger

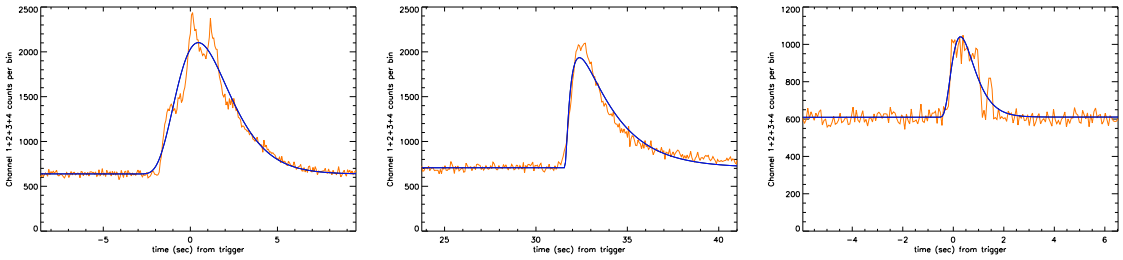
Channel 1+2+3+4 counts per bin
time (sec) from trigger
Channel 1+2+3+4 counts per bin
time (sec) from trigger
Channel 1+2+3+4 counts per bin
time (sec) from trigger

**Figure 13**. BATSE Trigger numbers used in the 27 Crown Summed Pulse. The first 13 of these pulses were the ones used to make up the 13 Crown Summed Pulse, 05339 05417 05448 : 05471 05527 05547 : 05607 05644 06307 : 06386 06697 06715 : 06757 07102 07191 : 07228 07290 07297 : 07298 07494 07504 : 07527 07663 07735 : 07822 07918 07939

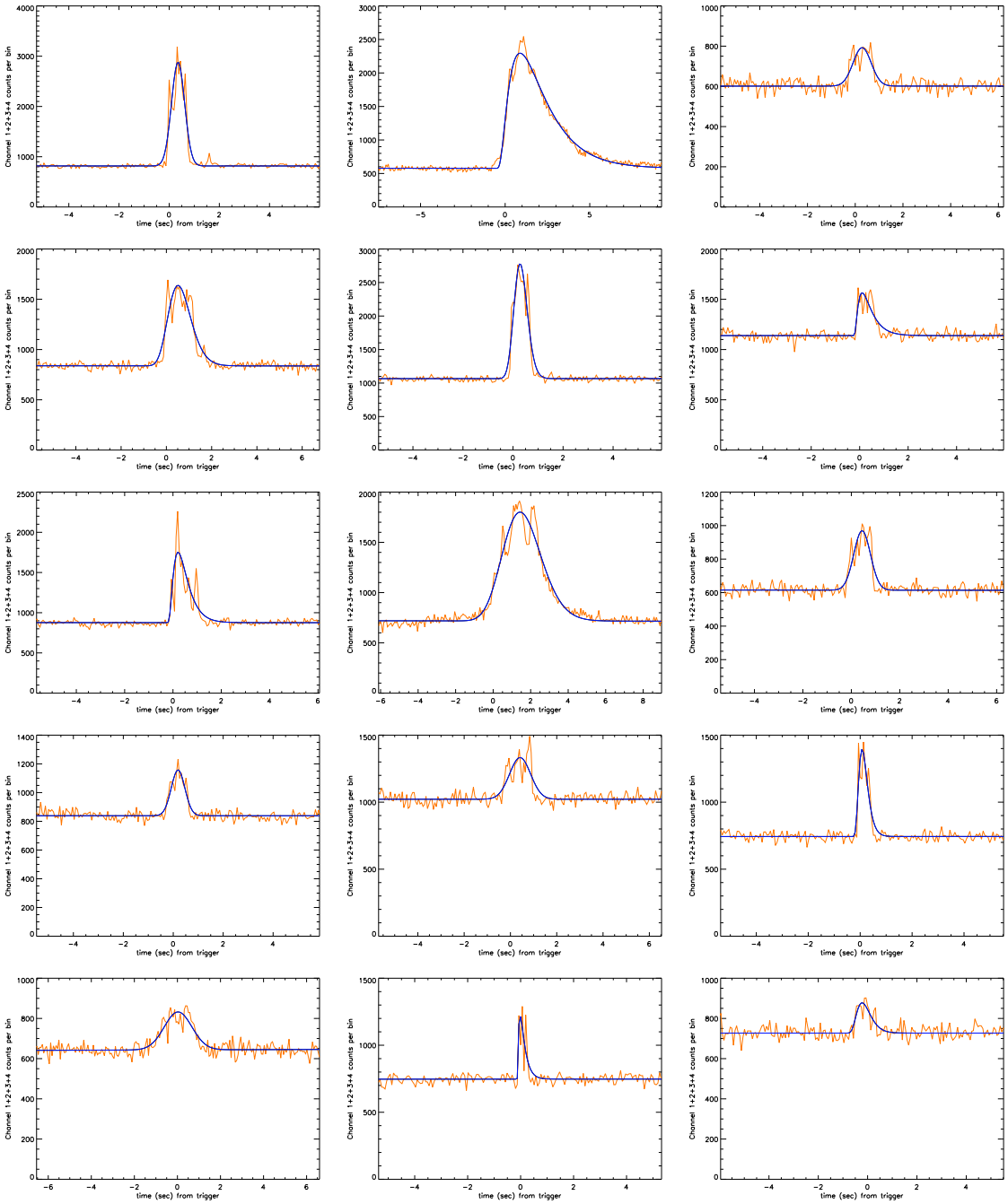

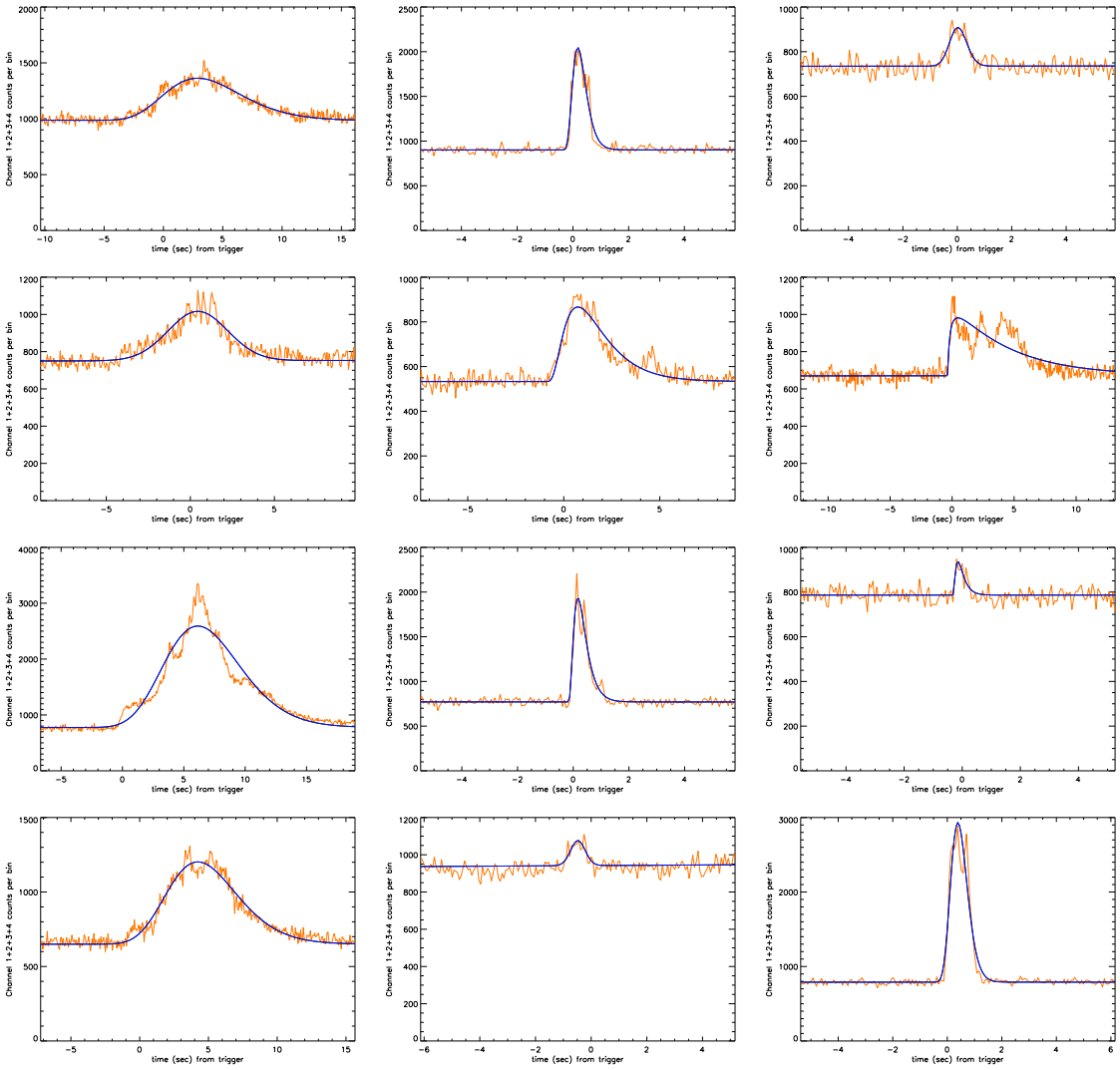
Channel 1+2+3+4 counts per bin
time (sec) from trigger

## REFERENCES


Costa, E., 1997, Nature, 387, 783-785.
Fishman, G. J., 1989, A&AS, 97, 1.
Hakkila, J., Giblin, T. W., Norris, J. P., et al. 2008, American Institute of Physics Conference Series, 1000, 109
Hakkila, J., & Preece, R. D., 2011, ApJ, 740, 104.
Hakkila, J., & Preece, R. D., 2014, ApJ, 783, 88.
Hakkila, J., Lien, A., Sakamoto, T., 2015, ApJ, 815, 134.
Klebesadel, R. W., 1973, ApJ, 182, L85.
Metzger, M. R., 1997, Nature, 387, 878-880.
Norris, J. P., 1997, Proceedings of the 25th ICRC
Norris, J. P., Bonnell, J.T., Kazanas, D., et al. 2005, ApJ, 627, 324-245.
Paciesas, W. S., 1999, ApJ, 122, 465.
Rees, M. J., & Meszaros, P., 1992, MNRAS, 253, 2.
Scargle, J. D., 1998, ApJ, 504, 405.